Composite Structures 131 (2015) 594–605

Contents lists available at ScienceDirect

Composite Structures

journal homepage: www.elsevier.com/locate/compstruct

Rotational and ply-level uncertainty in response of composite shallow conical shells

S. Dey [a,*], T. Mukhopadhyay [a], H. Haddad Khodaparast [a], P. Kerfriden [b], S. Adhikari [a]

[a] College of Engineering, Swansea University, United Kingdom
[b] Cardiff University, United Kingdom

ARTICLE INFO

Article history:
Available online 10 June 2015

Keywords:
Rotational uncertainty
Central composite design method
Natural frequency
Shallow conical shell
Sensitivity analysis
Stochastic mode shapes

ABSTRACT

This paper presents the quantification of rotational and ply level uncertainty of random natural frequency for laminated composite conical shells by using surrogate modeling approach. The stochastic eigenvalue problem is solved by using QR iteration algorithm. Sensitivity analysis is carried out to address the influence of different input parameters on the output natural frequencies. The sampling size and computational cost is reduced by employing the present approach compared to direct Monte Carlo simulation. The stochastic mode shapes are also depicted for a typical laminate configuration. Statistical analysis is presented to illustrate the results and its performance.

1. Introduction

Laminated composite shell structures are extensively used in aerospace, marine, automobile industries due to their high strength and stiffness to weight ratios. Modeling realistic composite structures is a numerically demanding task. However, turbomachinery blades such as wind turbine blades can be, as a first approximation, idealized as shallow conical shells in order to simplify the numerical simulation process. The production of shell-like structures is always subjected to large variability due to manufacturing imperfection and operational factors. Composite materials are difficult to manufacture accurately according to its exact design specifications resulting in unavoidable uncertainties. Typical uncertainties incurred are porosity, excess resin between plies, incomplete curing of resin, excess matrix voids, intra-laminate voids, variations in fiber parameters. For instance, the fiber orientation angle may vary due to lack of precision and accuracy to maintain the exact design specification for each layer of the laminate. The rotational speed of turbomachinery blades itself might be uncertain, varying in a range around its working speeds due to fluctuation of payload during operation. Even the lower ranges of rotational speeds for wind turbine blades are always subjected to large variability due to uncertain air velocity. In reality the blades of wind turbine do not rotate at constant speed rather rotate about their axis at variable rotational speeds which may lead to structural damage of the blades. Hence it results in unavoidable dynamic instability of the system caused due to variations of rotational speeds and ply-orientation angle. In general, additional factor of safety is assumed by the designers due to difficulty in quantifying those uncertainties. This existing practice of designer results in either an ultraconservative or an unsafe design. The variability in one input parameter may propagate and influence to another and the final output quantity (say random natural frequency) of the system may have a significant cascading effect due to accumulation of risk. Therefore, it is essential to estimate the variability in natural frequencies together with the expected performance characteristic value (say mean deterministic natural frequency) to ensure the operational safety.

The present model and algorithm is developed by using mathematical and statistical methods to obtain central composite design (CCD) [1,2] (illustrated in Section 3). The basis of design and analysis of experiments [3,4] are investigated extensively in the last two decades. In other studies found in the open literature, the CCD approach provides rotatable design for modeling and optimization of a multi-gravity separator for chromite concentration [5]. Fang and Perera [6] studied damage identification technique while Ahmadi et al. [7] investigated the advanced treatment of olive oil processing wastewater using Fenton's peroxidation and Zhu and Chen [8] studied the dynamic analysis of machine tool based on unit structure by employing CCD. Of late several studies are carried out concerning different deterministic responses of composite shells [9–20], while stochastic analysis of the same are found to be carried out in ref [21,22]. Mehrez et al. [23,24] investigated the stochastic material properties of composites by experimental database construction and uncertainty modeling. A stochastic multi-scale approach on composite is employed by using elastodynamic wave equation [25] while a statistical

* Corresponding author.
E-mail addresses: infosudip@gmail.com, S.Dey@swansea.ac.uk (S. Dey).

http://dx.doi.org/10.1016/j.compstruct.2015.06.011
0263-8223/

modeling for uncertainty quantification is used in frequency response function estimation [26]. The uncertainty quantification in dynamic responses of composite plates is investigated by Sepahvand et al. [27] and Dey et al. [28] while Jagtap et al. [29] studied the stochastic nonlinear free vibration analysis of elastically supported functionally graded materials plate with system randomness in thermal environment. The design of composite laminates is studied by a Monte Carlo method [30] while stochastic finite element method is employed for combined random material and geometric properties of composite shells [31]. The probabilistic approach is employed for stochastic modeling of fiber reinforced plastic composites [32], risk analysis [33] and interval of uncertainty [34] while it is also utilized in multi-scale noise tuning of resonance for enhanced fault diagnosis in rotating machines [35]. The dynamics of thin-walled composite beams is analyzed by parametric uncertainties [36]. The micromechanics of materials is studied with stochastic finite elements by Charmpis et al. [37] and the sensitivity of bistable laminates with uncertain geometric and material properties is investigated by Brampton et al. [38]. Salim et al. [39] studied the buckling characteristics of laminated plates with random material properties while Sarangapani et al. [40] investigated on spatial wavelet approach to local matrix crack detection in composite beams with ply level material uncertainty and Dimitrov et al. [41] carried out the reliability analysis of a composite wind turbine blade section using the model correction factor method. In general, Monte Carlo simulation technique is popularly utilized to generate uncertain random output frequencies dealing with large sample sizes. The uncertainty in material and geometric properties can be computed by direct Monte Carlo Simulation incurring high computational cost. To mitigate this lacuna, present analysis employed the CCD technique to map the uncertainties in a more efficient manner. Its purpose is to estimate response quantities (say natural frequency) based on randomness considered in input parameters (for instance, ply orientation angle and rotational speeds). The proposed procedure is based on constructing response surfaces. Those surfaces represent an estimate for the relationship between the input parameters of the numerical model of the structure and the quantities of interest.

The stochastic approach for uncertainty quantification of natural frequency of composite structures has gained attention but the treatment of rotational and ply level uncertainties for composite structures and their combined effect have not yet addressed. The novelty in the present study includes in quantifying the rotational and ply-level uncertainty and sensitivity for the first three natural frequencies of laminated composite conical shells. Moreover, to the best of authors' knowledge, the use of central composite design is the first attempt of its kind to apply in realm of stochastic analysis of laminated composites. In the present analysis, selective representative samples are drawn uniformly over the entire parameter domain, ensuring good prediction capability of the constructed meta-model in the whole design space including the tail regions. An algorithm is developed to quantify the uncertainties in natural frequencies of cantilever composite conical shells using the CCD technique and its efficiency is compared with direct Monte Carlo simulation (MCS). The sensitivity analysis is carried out to map the effect of the variation of individual input parameter on the quantities of interest by making use of the constructed meta-model. Subsequently the number of sample runs required to fit the constructed meta-model is drastically reduced. An eight noded isoparametric quadratic element with five degrees of freedom at each node is considered in the finite element formulation.

2. Governing equations

The orthotropic composite shallow conical shell with length L_O, reference width b, thickness t, semi-vertex angle ϕ_{ve} and base subtended angle of cone ϕ_o is depicted in Fig. 1. The component of radius of curvature in the chordwise direction $r_y(x,y)$ is a parameter varying both in the x- and y-directions. The variation in x-direction is linear. There is no curvature along the spanwise direction ($r_x = \infty$). The cantilever shell is clamped along $x = 0$ with radius of twist r_{xy}. Thus a shallow conical shell of uniform thickness, made of laminated composite is considered. A shallow shell is characterized by its middle surface and is defined by the equation,

$$z = -0.5[(x^2/r_x) + (2xy/r_{xy}) + (y^2/r_y)] \tag{1}$$

The radius of twist (r_{xy}), length (L_O) of the shell and twist angle (Ψ) are expressed as [42]

$$r_{xy} = -L_O/\tan\ \psi \tag{2}$$

The constitutive equations for composite conical shell are given by

$$\{F\} = [D(\overline{\omega})]\ \{\varepsilon\} \tag{3}$$

Here the symbol $(\overline{\omega})$ indicates the stochasticity of respective parameter.

where force resultant

$$\{F\} = \{\, N_x,\quad N_y,\quad N_{xy},\quad M_x,\quad M_y,\quad M_{xy},\quad Q_x,\quad Q_y \,\}^T \tag{4}$$

$$\{F\} = \left[\int_{-t/2}^{t/2} \{\, \sigma_x,\quad \sigma_y,\quad \tau_{xy},\quad \sigma_x z,\quad \sigma_y z,\quad \tau_{xy} z,\quad \tau_{xz},\quad \tau_{yz} \,\} dz\right]^T$$

$$\{\varepsilon\} = \{\, \varepsilon_x,\quad \varepsilon_y,\quad \varepsilon_{xy},\quad k_x,\quad k_y,\quad k_{xy},\quad \gamma_{xz},\quad \gamma_{yz} \,\}^T$$

and

$$[D(\overline{\omega})] = \begin{bmatrix} A_{ij}(\overline{\omega}) & B_{ij}(\overline{\omega}) & 0 \\ B_{ij}(\overline{\omega}) & D_{ij}(\overline{\omega}) & 0 \\ 0 & 0 & S_{ij}(\overline{\omega}) \end{bmatrix} \tag{5}$$

The elements of elastic stiffness matrix $[D(\overline{\omega})]$ is expressed as

$$[A_{ij}(\overline{\omega}), B_{ij}(\overline{\omega}), D_{ij}(\overline{\omega})] = \sum_{k=1}^{n} \int_{z_{k-1}}^{z_k} [\{\overline{Q}_{ij}(\overline{\omega})\}_{on-axis}]_k\, [1, z, z^2] dz \quad i,j = 1,2,6$$

$$[S_{ij}(\overline{\omega})] = \sum_{k=1}^{n} \int_{z_{k-1}}^{z_k} \alpha_s [\{\overline{Q}_{ij}(\overline{\omega})\}_{on-axis}]_k dz \quad i,j = 4,5 \tag{6}$$

where $[\overline{Q}_{ij}(\overline{\omega})]_{on-axis}$ is the on-axis elastic constant matrix, z_k denotes the distance of kth layer from the mid-plane of the laminate and α_s represents the shear correction factor which is assumed as 5/6. $[\overline{Q}_{ij}(\overline{\omega})]_{off-axis}$ is the off-axis elastic constant matrix which is given by

$$[\overline{Q}_{ij}(\overline{\omega})]_{off-axis} = [T_1(\overline{\omega})]^{-1} [\overline{Q}_{ij}]_{on-axis} [T_1(\overline{\omega})]^{-T} \quad \text{for} \quad i,j = 1,2,6$$

$$[\overline{Q}_{ij}(\overline{\omega})]_{off-axis} = [T_2(\overline{\omega})]^{-1} [\overline{Q}_{ij}]_{on-axis} [T_2(\overline{\omega})]^{-T} \quad \text{for} \quad i,j = 4,5 \tag{7}$$

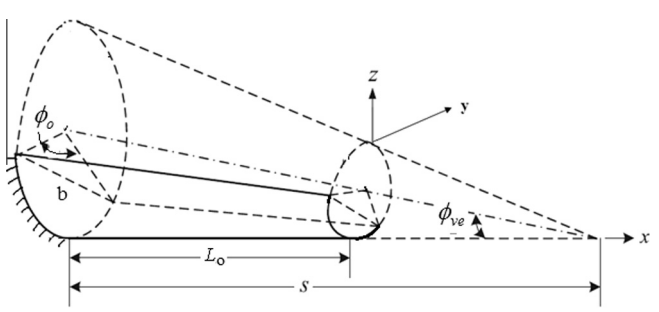

Fig. 1. Conical shell model.

where $[T_1(\overline{\omega})]$ and $[T_2(\overline{\omega})]$ are the transformation matrices and can be expressed as

$$[T_1(\overline{\omega})] = \begin{bmatrix} m^2 & n^2 & 2mn \\ n^2 & m^2 & -2mn \\ -mn & mn & m^2-n^2 \end{bmatrix} \quad \text{and} \quad [T_2(\overline{\omega})] = \begin{bmatrix} m & -n \\ n & m \end{bmatrix} \tag{8}$$

in which $m = Sin\theta(\overline{\omega})$ and $n = Cos\theta(\overline{\omega})$, wherein $\theta(\overline{\omega})$ is random ply orientation angle,

$$[Q_{ij}(\overline{\omega})]_{on-axis} = \begin{bmatrix} Q_{11} & Q_{12} & 0 \\ Q_{12} & Q_{12} & 0 \\ 0 & 0 & Q_{66} \end{bmatrix} \quad \text{for} \quad i,j = 1,2,6 \tag{9}$$

$$[\overline{Q}_{ij}(\overline{\omega})]_{on-axis} = \begin{bmatrix} Q_{44} & Q_{45} \\ Q_{45} & Q_{55} \end{bmatrix} \quad \text{for} \quad i,j = 4,5 \tag{10}$$

where in Q_{ij} are obtained by definition of orthotropic material considered for conical shells as follows,

$$Q_{11} = \frac{E_1}{1-\nu_{12}\nu_{21}}, \quad Q_{22} = \frac{E_2}{1-\nu_{12}\nu_{21}} \quad \text{and} \quad Q_{12} = \frac{\nu_{12}E_2}{1-\nu_{12}\nu_{21}}$$

$$Q_{66} = G_{12} \quad Q_{44} = G_{23} \quad \text{and} \quad Q_{55} = G_{13}$$

The mass per unit area for conical shell is expressed as

$$P(\overline{\omega}) = \sum_{k=1}^{n} \int_{z_{k-1}}^{z_k} \rho(\overline{\omega}) dz \tag{11}$$

Mass matrix is expressed as

$$[M(\overline{\omega})] = \int_{Vol} [N][P(\overline{\omega})][N] d(vol) \tag{12}$$

The stiffness matrix is given by

$$[K(\overline{\omega})] = \int_{-1}^{1}\int_{-1}^{1} [B(\overline{\omega})]^T [D(\overline{\omega})][B(\bar{\omega})] d\xi d\eta \tag{13}$$

where ξ and η are the local natural coordinates of the element. From Hamilton's principle [43], the dynamic equilibrium equation for rotational speeds is derived by employing Lagrange's equation of motion and neglecting Coriolis effect. The equation in global form is subsequently expressed as [44–46]

$$[M(\overline{\omega})]\{\ddot{\delta}_e\} + ([K_e(\overline{\omega})] + [K_{ce}(\overline{\omega})]\{\delta_e\} = \{F_e(\overline{\omega})\} + \{F_{ce}(\overline{\omega})\} \tag{14}$$

where $[M(\overline{\omega})]$, $[K_e(\overline{\omega})]$ and $[K_{ce}(\overline{\omega})]$ are the mass, element elastic stiffness, element geometric stiffness matrices, respectively while $\{F_e(\overline{\omega})\}$ and $\{F_{ce}(\overline{\omega})\}$ represent the vectors for element externally applied force and element centrifugal force, respectively and $\{\delta_e\}$ denotes the vector of element generalized coordinates. After assembling all the element matrices and the force vectors with respect to the common global coordinates, the equation of motion of a free vibration system with n degrees of freedom can be expressed as

$$[M(\overline{\omega})][\ddot{\delta}] + [K_e(\overline{\omega}) + K_{\sigma e}(\overline{\omega})]\{\delta\} = \{F\} + \{F(\Omega^2)\} \tag{15}$$

In the above equation, $(M\overline{\omega}) \in R^{n\times n}$ is the mass matrix, $[(K\overline{\omega})]$ is the stiffness matrix wherein $[K(\overline{\omega})] = [K_e(\overline{\omega})] + [K_{\sigma e}(\overline{\omega})]$ in which $K_e(\overline{\omega}) \in R^{n\times n}$ is the elastic stiffness matrix, $K_{\sigma e}(\overline{\omega}) \in R^{n\times n}$ is the geometric stiffness matrix (depends on initial stress distribution) while $\{\delta\} \in R^n$ is the vector of generalized coordinates and $\{F\} \in R^n$ is the externally applied force vector. $\{F(\Omega^2)\}$ is the vector of nodal equivalent centrifugal forces, $\{F\}$ is the global vector of externally applied force and $\{\delta\}$ is the global displacement vector. $[K_\sigma]$ depends on the initial stress distribution and is obtained by the iterative procedure upon solving

$$(K_e(\overline{\omega}) + K_\sigma(\overline{\omega}))\{\delta\} = \{F(\Omega^2)\} \tag{16}$$

Angular velocity matrix components contributing towards acceleration vector is given as [47]

$$[A_o(\overline{\omega})] = \begin{bmatrix} \{\sigma_y^2(\overline{\omega}) + \sigma_z^2(\overline{\omega})\} & -\sigma_x(\overline{\omega})\sigma_y(\overline{\omega}) & -\sigma_x(\overline{\omega})\sigma_z(\overline{\omega}) \\ -\sigma_x(\overline{\omega})\sigma_y(\overline{\omega}) & \{\sigma_x^2(\overline{\omega}) + \sigma_z^2(\overline{\omega})\} & -\sigma_y(\overline{\omega})\sigma_z(\overline{\omega}) \\ -\sigma_x(\overline{\omega})\sigma_z(\overline{\omega}) & -\sigma_y(\overline{\omega})\sigma_z(\overline{\omega}) & \{\sigma_x^2(\overline{\omega}) + \sigma_y^2(\overline{\omega})\} \end{bmatrix} \tag{17}$$

The element centrifugal force is given by

$$[F_{ce}(\overline{\omega})] = \rho \int_V [N]^T [A_o(\overline{\omega})] \begin{bmatrix} t_x + x \\ t_y + y \\ t_z + z \end{bmatrix} dV \tag{18}$$

where $\{\rho\}$ is the mass density, $[N]$ stands for the shape function matrix and $\{t_x, t_y, t_z\}$ are the fixed translational offsets expressed with respect to the plate coordinate system. The element geometric stiffness matrix due to rotation is given by [48]

$$[K_{ce}(\overline{\omega})] = \int_V [G]^T [M_\sigma(\overline{\omega})][G] dV \tag{19}$$

where the matrix $[G]$ consists of derivatives of shape functions and $[M_\sigma(\overline{\omega})]$ is the matrix of initial in-plane stress resultants caused by rotation. Considering randomness of input parameters like ply-orientation angle, mass density, rotational speeds, the equation of motion of free vibration system with n degrees of freedom can be expressed as

$$[M(\overline{\omega})][\ddot{\delta}] + [K(\overline{\omega})]\{\delta\} = \{F_L\} \tag{20}$$

The governing equations are derived based on Mindlin's theory incorporating rotary inertia, transverse shear deformation. For free vibration, the random natural frequencies $[\omega_n(\overline{\omega})]$ are determined from the standard eigenvalue problem [49] which is represented below and is solved by the QR iteration algorithm,

$$[A(\overline{\omega})]\{\delta\} = \lambda(\overline{\omega})\{\delta\} \tag{21}$$

where

$$[A(\overline{\omega})] = ([K_e(\overline{\omega})] + [K_{\sigma e}(\overline{\omega})])^{-1}[M(\overline{\omega})]$$

$$\lambda(\overline{\omega}) = \frac{1}{\{\omega_n(\overline{\omega})\}^2} \tag{22}$$

3. Surrogate model – central composite design

A surrogate model is a mathematical and statistical approximation of a detailed and usually computationally expensive simulation model. The metamodels can be used as surrogates of the actual model when a large number of evaluations are needed. Formation of a surrogate model is typically three-step process. First step is the selection of representative sample points using design of experiment (DOE) concept. In the second step, outputs or responses are evaluated corresponding to each sample point obtained. After obtaining the set of design points and corresponding responses, the last step is the formation of metamodel to map the input–output relationship. Several sampling techniques (such as, Factorial designs, Central composite design, Optimal design, Taguchi's orthogonal array design, Plackett–Burman designs, Koshal designs, Box-Behnken design, Latin hypercube sampling, sobol sequence) [1,50–52] and metamodel formation method (such as, Polynomial regression method, Moving least squares method, Kriging, Artificial neural networks, Radial basis function, Multivariate adaptive regression splines, Support vector regression, High dimensional model representation) [21,53–55] exist. One of the main concerns is the selection of appropriate DOE method and metamodelling technique for a particular problem.

All the sampling methods and metamodelling techniques have their unique properties and there exists no universal model that can be regarded as the best choice for all types of problems. Sampling method and metamodelling technique for a particular problem should be chosen depending on the complexity of the model, presence of noise in sampling data, nature and dimension (number) of input parameters, desired level of accuracy and computational efficiency. Before using a particular metamodelling technique it is essential to check rigorously for its quality of fitting and prediction capability. Many comparative studies have been performed over past two decades to guide the selection of metamodel types [56–59]. A concise review of these studies conclude that though particular technique tends to perform better for a particular type of problem involving high level of complexity depending on its nature, most of the metamodelling techniques work satisfactorily for simple linear models. Polynomial regression technique based on central composite design has been established as one of the simplest and most efficient methods through its wide range of application [5–8,60,61]. Application of central composite design for metamodel formation in the area of structural engineering and mechanics (specifically in FRP composite structures) is still very scarce, in spite of the fact that it has an immense potential to be used as surrogate of expensive finite element simulation or experimentations of repetitive nature. Central composite design method can be employed for composite structures wherein large number of input parameters can be efficiently analyzed. The present problem is considered as linear in nature and the sampling data is noise free. In this analysis, a central composite design is used to construct a polynomial regression model for the first three natural frequencies. The statistical measure of goodness of a model is obtained by least squares regression analysis for the minimum generalized variance of the estimates of the model coefficients. Considering the problem of estimating the coefficients of the model by least squares regression analysis

$$y = \beta_o + \sum_{i=1}^{k} \beta_i x_i + \varepsilon \tag{23}$$

In matrix form the above equation can be expressed as

$$Y = X\beta + \varepsilon \tag{24}$$

where 'Y' is a vector of observations of sample size, 'ε' is the vector of errors having normal distribution with zero mean, 'X' is the design matrix and 'β' is a vector of unknown model coefficients (βo and βi). The design matrix is a set of combinations of the values of the coded variables, which specifies the settings of the design parameters to be performed during data observation. In CCD, the following three portions are considered for obtaining design points: a complete (or a fraction of) 2^k factorial design coded as ±1 (corresponding to the lower and upper value bound of the design space) consisting of 2^k design points, $2k$ axial points coded as $\pm\alpha$ ($\alpha \geqslant 1$) and n_0 center points as shown in Fig. 2. Here 'k' is the number of input variables. Thus the total number of design points in CCD model, $n = 2^k + 2k + n_0$ where $n_0 = 1$ for present numerical study. CCD possesses the following properties according to the chosen values of α and n_0 [1,4]:

(a) Rotatable (used for up to 5 factors to creates a design with standard error of predictions equal at points equidistant from the center of the design)
(b) Face-centred (the axial points into the faces of the cube at ±1 levels to produce a design with each factor having 3 levels)
(c) Spherical (all factorial and axial points on the surface of a sphere of radius equals to square root of the number of factors)
(d) Orthogonal quadratic (α values allowing the quadratic terms to be independently estimated from the other terms)
(e) Practical (used for 6 or more factors wherein α value is the fourth root of the number of factors)

If the number of input parameters (k) is more than 5, the 2^k design requires a large number of design points which is encountered by employing either one-half fraction design (consisting of one-half the number of points) or one-fourth fraction design (consisting of one- fourth the number of points). In general, a 2^{-m} th fraction of a 2^k design consists of 2^{k-m} points from a full 2^k design wherein m is chosen in such a way that $2^{k-m} \geqslant$ number of unknowns in the response surface equation.

In the present study, the constructed CCD models provide an approximate meta-model which relates the input random parameters 'x_i' (say ply orientation angle of each layer of laminate, rotational speed) and output 'y' (say natural frequency)

$$y = f(x_1, x_2, x_3, x_4, \ldots x_i \ldots x_k) + \varepsilon \tag{25}$$

where 'f' denotes the approximate response function, 'ε' is the statistical error term having a normal distribution with null mean value. The input variables are usually coded as dimensionless variables with zero as mean value and a standard deviation of 'x_i'. The first order and second order polynomials are expressed as

First order model (interaction),

$$y = \beta_o + \sum_{i=1}^{k} \beta_i x_i + \sum_{i=1}^{k} \sum_{j>i}^{k} \beta_{ij} x_i x_j + \varepsilon \tag{26}$$

Second order model,

$$y = \beta_o + \sum_{i=1}^{k} \beta_i x_i + \sum_{i=1}^{k} \sum_{j>i}^{k} \beta_{ij} x_i x_j + \sum_{i=1}^{k} \beta_{ii} x_i^2 + \varepsilon \tag{27}$$

The surrogate model is used to fit approximately for a set of points in the design space using a multiple regression fitting scheme. While forming CCD models, insignificant input features are screened out and not considered in the final meta-model. A quantitative evaluation for effect of each parameter on the total model variance is carried out using analysis of variance (ANOVA) method according to its F-test value

$$F_p = \frac{n-k-1}{k}\left(\frac{SS_R}{SS_E}\right) \tag{28}$$

where F_p denotes the F-test value of any input parameter 'p' while n, SS_E and SS_R are the number of samples used in the design procedure, sum of squares due to the model and the residual error, respectively. If F_p exceeds the selected criterion value, the input parameter 'p' is considered to be significantly influencial factor with respect to the chosen output feature. The percentage contribution of each input parameter (including the contribution of the interaction terms) to the total model variance is obtained for each input random variables for each layer of laminated composite conical shells. An optimized surrogate model is formed by adding or deleting input factors through backward elimination, forward addition or stepwise elimination or addition. It involves the calculation of the P-value (probability value, gives the risk of falsely rejecting a given hypothesis) and $Prob. > F$ value (gives the proportion of time one would expect to get the stated F-value if no factor effects are significant). The meta-model constructed is checked by two basic criteria such as coefficient of determination or R^2 term (measure of the amount of variation around the mean explained by the model) and R^2_{adj} term (measure of the amount of variation with respect to mean value explained by the model, adjusted for the number of terms in the model). The adjusted R^2 decreases as the number of terms in the model increases if those additional terms do not add value to the model) and R^2_{pred} (measure of the prediction capability of the response surface model) expressed as follows.

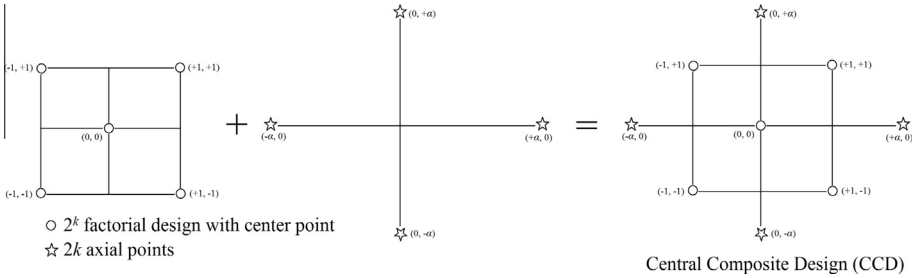

Fig. 2. Central composite design with two factors.

$$R^2 = \left(\frac{SS_R}{SS_T}\right) = 1 - \left(\frac{SS_E}{SS_T}\right) \quad \text{where} \quad 0 \leqslant R^2 \leqslant 1 \tag{29}$$

$$R^2_{adj} = 1 - \frac{\left(\frac{SS_E}{n-k-1}\right)}{\left(\frac{SS_T}{n-1}\right)} = 1 - \left(\frac{n-1}{n-k-1}\right)(1-R^2) \quad \text{where} \quad 0 \leqslant R^2_{adj} \leqslant 1 \tag{30}$$

$$R^2_{pred} = 1 - \left(\frac{PRESS}{SS_T}\right) \quad \text{where} \quad 0 \leqslant R^2_{pred} \leqslant 1 \tag{31}$$

where $SS_T = SS_E + SS_R$ is the total sum of square and *PRESS* (predicted residual error sum of squares) measures the goodness of fit of the model corresponding to chosen samples in the design space. In the present study, the stochasticity of ply-orientation angle in each layer of laminate and rotational speeds as input parameters are considered for composite cantilever conical shells. Fig. 3 presents the flowchart of stochastic natural frequency by using central composite design. It is assumed that the distribution of randomness of input parameters exists within a certain band of tolerance with their central deterministic mean values. The cases wherein the random variables considered in each layer of laminate are investigated for

(a) Variation of ply-orientation angle only:

$$\theta(\overline{\omega}) = \{\theta_1\, \theta_2\, \theta_3 \ldots \theta_i \ldots \theta_l\}$$

(b) Variation of mass density only:

$$\Omega(\overline{\omega})$$

(c) Combined variation of ply orientation angle and rotational speeds:

$$g\{\theta(\overline{\omega}), \Omega(\overline{\omega})\} = \{\Phi_1(\theta_1 \ldots \theta_l), \Phi_2(\Omega)\}$$

where θ_i and Ω_i are the ply orientation angle and rotational speed, respectively and '*l*' denotes the number of layer in the laminate. In present study, $\pm 5^\circ$ for ply orientation angle with subsequent $\pm 10\%$ tolerance for rotational speeds respectively from deterministic mean value are considered.

4. Results and discussion

The present study considers an eight layered graphite-epoxy symmetric angle-ply $(\theta^\circ/-\theta^\circ/\theta^\circ/-\theta^\circ)s$ composite cantilever shallow conical shells with a square plan-form ($L/b_o = 1$), curvature ratio (b_o/R_y) of 0.5 and thickness ratio of 1000. Material properties of graphite–epoxy composite [62] are considered with mean value as $E_1 = 138$ GPa, $E_2 = 8.96$ GPa, $\nu = 0.3$, $G_{12} = G_{13} = 7.1$ GPa, $G_{23} = 2.84$ GPa, $\rho = 3202$ kg/m^3. A typical discretization of (6×6) mesh on plan area with 36 elements 133 nodes with natural coordinates of an isoparametric quadratic plate bending element are considered for the present finite element model. For full scale MCS, number of original finite element analysis is the same as the sampling size. In general for complex composite structures, the performance function is not available as an explicit function of the random design variables. The random response in terms of natural frequencies of the composite structure can only be evaluated numerically at the end of a structural analysis procedure such as the finite element method which is often time-consuming. The present CCD is employed to find a predictive and representative meta-model equation by using one-half fraction design. The meta-models are used to determine the first three natural frequencies corresponding to given values of input variables, instead of time-consuming deterministic FE analysis. The response surface thus represents the result (or output) of the structural analysis encompassing (in theory) every reasonable combination of all input variables. Due to paucity of space, only a few important representative results are furnished.

4.1. Validation

The present computer code is validated with the results available in the open literature. Table 1 presents the non-dimensional fundamental frequencies of isotropic and homogeneous untwisted shallow conical shells [42]. The convergence study is carried out to determine the natural frequencies for composite conical shells. Table 2 presents the non-dimensional fundamental frequencies of graphite-epoxy composite rotating cantilever plate [45]. In computer code, shell to plate transformation is done by assuming a large value of radius of curvatures ($\sim 20 \times 10^{20}$) compared to its length or width or thickness. In Tables 1 and 2, the geometry and material properties are considered with respect to Refs. [42] and [60], respectively. The mesh division of (4×4), (6×6) and (8×8) are employed for convergence study wherein the downward monotonic convergence is observed. Around 1% difference is found between the results obtained by present analysis and that of Liew et al. [42]. The effect of rotary inertia and transverse shear deformation influences such difference with a control on overestimation the structural stiffness of composite conical shells. In the present study, mesh size of (6×6) is adopted to reduce the cost of computation. The comparative study depicts an excellent agreement with the previously published results and hence it demonstrates the capability of the computer codes developed and ensures the accuracy of analyses. In CCD, a representative sample size of 150 is considered for each layer's of individual variation of ply-orientation angle and rotational speeds, respectively. Due to increase in number of input variables considered for combined random variation of ply-orientation angle and rotational speeds, the subsequent sample size of 280 is adopted to meet the convergence criteria. Fig. 4 depicts a representative plot describing the relationship between the original finite element model and the constructed CCD meta-model for fundamental natural frequencies signifying the accuracy of the present meta-model. Fig. 5 illustrates the comparison of the probability density functions (PDF) for both original MCS and CCD using sample size of 10,000 corresponding to

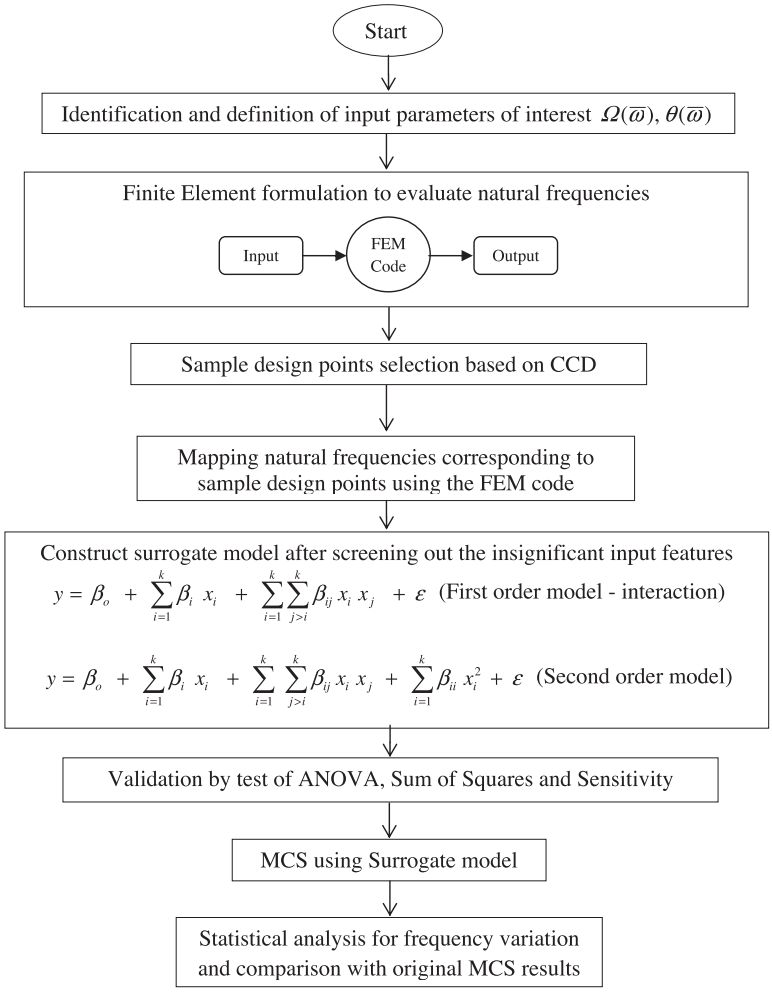

Fig. 3. Flowchart of stochastic natural frequency using central composite design.

Table 1
Non-dimensional fundamental frequencies [$\omega = \omega_n b^2 \sqrt{(\rho t/D)}$, $D = Et^3/12(1-\nu^2)$] for isotropic and homogeneous untwisted shallow conical shells with $\nu = 0.3$, $s/t = 1000$, $\phi_o = 30°$, $\phi_{ve} = 15°$.

Aspect ratio (L/s)	Present FEM (4 × 4)	Present FEM (6 × 6)	Present FEM (8 × 8)	Liew et al. [42]
0.6	0.3541	0.3552	0.3524	0.3599
0.7	0.2995	0.3013	0.2991	0.3060
0.8	0.2729	0.2741	0.2715	0.2783

Table 2
Non-dimensional fundamental frequencies [$\omega = \omega_n L^2 \sqrt{(\rho t/D)}$] of graphite-epoxy composite rotating cantilever plate, $L/b_o = 1$, $t/L = 0.12$, $D = E t^3/\{12(1-\nu^2)\}$, $\nu = 0.3$.

Ω	Present FEM	Sreenivasamurthy and Ramamurti [47]
0.0	3.4174	3.4368
1.0	4.9549	5.0916

first three natural frequencies considering individual as well as combined variation of ply orientation angle, rotational speed. The low scatterness of the points found around the diagonal line in Fig. 4 and the low deviation obtained between the pdf estimations of original MCS and CCD responses in Fig. 5 corroborates the fact that CCD meta-models are formed accurately. These two plots are checked and are found in good agreement ensuring the efficiency and accuracy of the present constructed CCD. While evaluating the statistics of responses through full scale MCS, computational time is exorbitently high because it involves number of repeated FE analysis. However, in the present method, MCS is conducted in conjunction with CCD model. Here, although the same sampling size as in direct MCS (with sample size of 10,000) is considered, the number of FE analysis is much less compared to original MCS and is equal to number representative sample required to construct the CCD meta-model. The representative CCD equation is formed on which the full sample size of direct MCS is conducted. Hence, the computational time and effort expressed in terms of finite element calculation is reduced compared to full scale direct MCS. Hence, in order to save computational time, the present constructed CCD methodology is employed instead of traditional Monte Carlo simulation. This provides an efficient affordable way for simulating the uncertainties in natural frequency. The sensitivity of a given material or geometric property to each random variable is also quantified in the present meta-model context. The representative probability density function for angle-ply laminate with respect to stochastic input parameters are compared with the results predicted by a Monte Carlo simulation (10,000 samples) wherein a good agreement is observed as furnished in Fig. 5. In the present analysis, the values of R^2, R^2_{adj} and. are found to be close to one ensuring the best fit. The difference between R^2_{adj} and R^2_{pred} is found less than 0.2 which indicates that the model

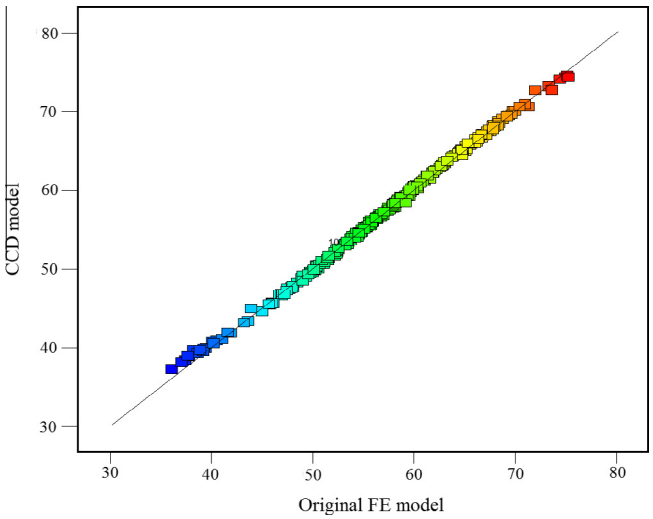

Fig. 4. Central composite design (CCD) model with respect to Original FE model of fundamental natural frequencies for combined variation of rotational speed and ply-orientation angle of angle-ply [(45°/−45°/45°/−45°)s] composite cantilever conical shells, considering E_1 = 138 GPa, E_2 = 8.9 GPa, $G_{12} = G_{13}$ = 7.1 GPa, G_{23} = 2.84 GPa, ρ = 3202 kg/m^3, t = 0.003 m, ν = 0.3, Lo/s = 0.7, ϕ_o = 45°, ϕ_{ve} = 20°.

can be used for further prediction. In addition to above, another check is carried out namely, adequate precision which compares the range of the predicted values at the design points to the average prediction error. For all cases of present CCD meta-model, its value is consistently found greater than four which indicates the present model is adequate to navigate the design space. The computational time required in the present CCD approach is observed to be around (1/67) times (for individual variation of inputs) and (1/35) times (for combined variation of inputs) of direct Monte Carlo simulation.

4.2. Statistical analysis

The variation of rotational speeds [$\Omega(\overline{\omega})$] ranging from 25 rpm to 125 rpm in step of 25 rpm are scaled randomly in the range having the lower and the upper limit as ±10% variability (as per industry standard manufacturing tolerance) with respective mean values while for ply orientation angle [$\theta(\overline{\omega})$] ranging from 0° to 90° in step of 15° in each layer of the composite laminate the bound is considered as within ±5° fluctuation (as per industry standard manufacturing tolerance) with respective mean deterministic values. The CCD meta-models are formed to generate first three natural frequencies for graphite-epoxy composite cantilever conical shells. The natural frequencies of tested angle-ply laminate are found to be reduced as the ply orientation angle increases irrespective of rotational speeds. Table 3 indicates the maximum values, minimum values, mean values and standard deviation for first three natural frequencies obtained due to individual and combined stochaticity in ply-orientation angle and rotational speeds for eight layered graphite-epoxy angle-ply composite conical shells wherein the results obtained using original MCS and CCD are observed to be in good agreement. Due to cascading effect of variability resulting from combined stochasticity considered in nine input parameters in each layer, the bandwidth of variation of natural frequency is found to be higher than the stochasticity considered for variation of any individual input parameter. Considering individual stochasticity in ply orientation angle [$\theta(\overline{\omega})$] and rotational speed [$\Omega(\overline{\omega})$], parametric study is carried out for maximum values, minimum values, means and standard deviations of first three natural frequencies as furnished in Tables 4 and 5, respectively. In general, the stochastic natural frequencies and its volatility are found to decrease with increase of fiber orientation angle and rotational speeds. Fig. 6 presents the sensitivity (in percentage) of natural frequencies with respect to ply orientation angle for eight layered graphite-epoxy angle-ply composite conical shells. Based on the sensitivity analysis using CCD the significant input parameter are

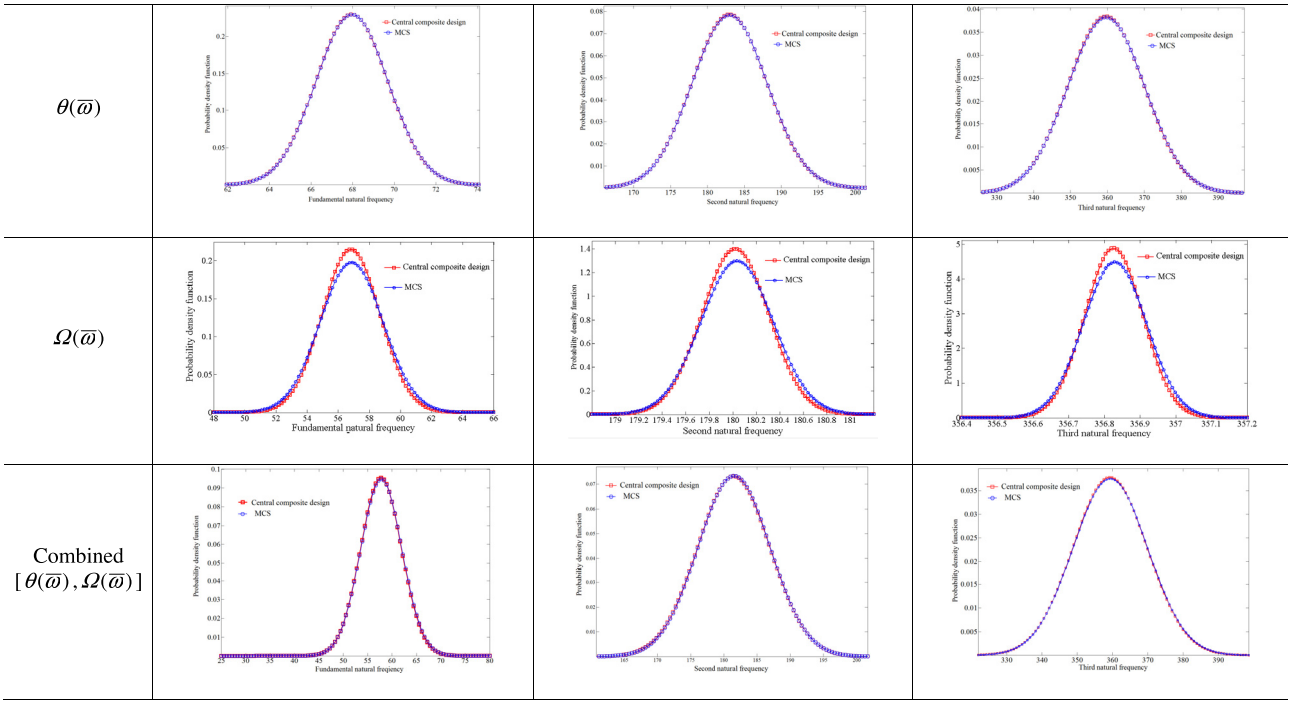

Fig. 5. Probability density function obtained by original MCS and Central composite design (CCD) with respect to first three natural frequencies (rad/s) indicating for variation of only ply orientation angle [$\theta(\overline{\omega})$], only rotational speeds [$\Omega(\overline{\omega})$] and combined [$\theta(\overline{\omega})$,$\Omega(\overline{\omega})$] for graphite-epoxy angle-ply [(θ°/−θ°/θ°/−θ °)s] composite conical shells, considering sample size = 10,000, θ = 45° (± 5° variation), $\Omega(\overline{\omega})$ = 100 rpm (with ± 10% variation), t = 0.003 m, ν = 0.3, Lo/s = 0.7, ϕ_o = 45°, ϕ_{ve} = 20°.

Table 3
Comparative study between MCS (10,000 samples) and Central composite design results for maximum values, minimum values and percentage of deviation for first three natural frequencies (rad/s) obtained for four layered graphite-epoxy angle-ply $[(\theta^\circ/-\theta^\circ/\theta^\circ/-\theta^\circ)s]$ composite conical shells considering $t = 0.003$ m, $v = 0.3$, $\theta = 45^\circ$ ($\pm$ 5° variation), $\Omega = 100$ rpm ($\pm$ 10% variation), $Lo/s = 0.7$, $\phi_o = 45^\circ$, $\phi_{ve} = 20^\circ$.

Parameter	Type of analysis	$[\theta(\overline{\omega})]$			$[\Omega(\overline{\omega})]$			$[\theta(\overline{\omega}),\Omega(\overline{\omega})]$		
		FNF	SNF	TNF	FNF	SNF	TNF	FNF	SNF	TNF
Max. value	MCS	73.9836	201.0528	396.413	59.92618	180.5032	356.9618	69.34976	201.2482	397.9168
	CCD	73.9588	201.003	396.294	59.62804	180.442	356.9445	68.2373	200.4119	396.5191
	Deviation (%)	0.033	0.025	0.030	0.498	0.034	0.005	1.604	0.416	0.351
Min value	MCS	62.0268	166.3178	326.3826	52.83288	179.4259	356.6496	32.09585	163.0662	326.0832
	CCD	62.0353	166.3642	326.4586	53.14518	179.4583	356.663	32.41708	161.1799	322.6536
	Deviation (%)	−0.014	−0.028	−0.023	−0.591	−0.018	−0.004	−1.001	1.157	1.052
Mean value	MCS	67.9652	182.9898	359.6682	56.86125	180.0369	356.8293	57.79991	181.5352	359.3835
	CCD	67.9545	182.9665	359.6045	56.82357	180.0214	356.826	57.74899	181.4775	359.2861
	Deviation (%)	0.016	0.013	0.018	0.066	0.009	0.001	0.088	0.032	0.027
Standard Deviation	MCS	1.7401	5.0895	10.4315	2.0162	0.3067	0.0888	4.206369	5.435023	10.6258
	CCD	1.7386	5.0742	10.3890	1.8555	0.2843	0.0814	4.178373	5.452521	10.54578
	Deviation (%)	0.089	0.299	0.407	7.973	7.292	8.231	0.666	−0.322	0.753

Table 4
Maximum value, minimum value, mean value and standard deviation (SD) of first three natural frequencies (rad/s) obtained by central composite design method (10,000 samples) due to individual stochaticity of ply-orientation angle in each layer for graphite-epoxy angle-ply $[(\theta^\circ/-\theta^\circ/\theta^\circ/-\theta^\circ)s]$ ($\pm$ 5° variation) composite conical shells, considering $t = 0.003$ m, $v = 0.3$, $Lo/s = 0.7$, $\phi_o = 45^\circ$, $\phi_{ve} = 20^\circ$.

$\theta(\overline{\omega})$	Fundamental natural frequency (FNF)				Second natural frequency (SNF)				Third natural frequency (TNF)			
	Max	Min	Mean	SD	Max	Min	Mean	SD	Max	Min	Mean	SD
0	134.841	120.913	128.9257	2.2486	399.0981	366.6211	389.0579	5.2026	766.6234	706.74	750.1372	9.7164
15°	125.885	116.052	121.2905	1.5321	367.722	333.234	351.1758	6.2208	711.5098	642.9308	678.387	12.4653
30°	104.396	90.0987	97.2914	2.1967	290.5747	243.7575	267.4248	7.2909	568.6029	476.5848	523.2368	14.4622
45°	73.9588	62.0353	67.95457	1.7386	201.003	166.3642	182.9665	5.0742	396.294	326.4586	359.6045	10.3890
60°	53.1915	47.4424	50.3265	0.9014	142.902	127.1338	134.8277	2.4918	280.4437	248.5910	263.7762	5.1014
75°	43.6186	41.2282	42.3783	0.3816	117.1097	111.0909	113.8941	0.9490	228.7734	216.8533	222.3898	1.8849
90°	40.3862	39.8526	40.0995	0.0874	108.9529	107.9854	108.3816	0.1629	212.6769	210.8513	211.5691	0.3058

Table 5
Central composite design results (10,000 samples) for first three natural frequencies (rad/s) due to stochaticity of rotational speeds $[\Omega(\overline{\omega})]$ (in rpm with $\pm$ 10% variation) for angle-ply $[(45^\circ/-45^\circ/45^\circ/-45^\circ)s]$ conical shells considering $t = 0.003$ m, $v = 0.3$, $Lo/s = 0.7$, $\phi_o = 45^\circ$, $\phi_{ve} = 20^\circ$.

$\Omega(\overline{\omega})$	Fundamental natural frequency				Second natural frequency				Third natural frequency			
	Max	Min	Mean	SD	Max	Min	Mean	SD	Max	Min	Mean	SD
0	–	–	67.4010 (deterministic)	–	–	–	181.5862 (deterministic)	–	–	–	357.2181 (deterministic)	–
25	67.2203	66.5726	66.9462	0.1887	181.5603	181.4726	181.5238	0.0255	357.2043	357.1882	357.1963	0.0046
50	66.2054	64.7281	65.5373	0.4263	181.4266	181.2223	181.3356	0.0591	357.1790	357.1367	357.1592	0.0122
75	64.0176	61.1246	62.7071	0.8332	181.1034	180.6880	180.9182	0.1200	357.1081	357.0063	357.0626	0.0294
100	59.6280	53.1451	56.8235	1.8555	180.4420	179.4583	180.0214	0.2844	356.9445	356.6630	356.8260	0.0815
125	52.6861	39.8621	46.2973	3.6973	178.4963	177.1830	177.6214	0.3919	356.3245	355.9771	356.0645	0.0969

screened. The effect of individual stochasticity of ply orientation angle at each layer of laminate is numerically investigated for angle-ply $[(\theta^\circ/-\theta^\circ/\theta^\circ/-\theta^\circ)s]$ composite conical shells wherein the sensitivity of two outermost layers (i.e., layer 1 and layer 8) are found to be maximum for $\theta = 0^\circ$, 15°, 30° and 90° while immediate underneath layers (i.e., layer 2 and layer 7) of the two outermost layers are observed to be maximum sensitive for $\theta = 45^\circ$, 60° and 75°. This is due the fact that only bending modes are predominant which results in maximum strains at outer layers. This consequently make the sensitively of natural frequencies with respect to fiber angles more sensitive at outmost layers. A complementary effect in sensitivity is identified between ultimate and penultimate outer layers corresponding to all ply orientation angles. In contrast, the two middle layers (i.e., layer 4 and layer 5) are found to be least sensitive for first three natural frequencies considering individual stochasticity of ply-orientation angle. Hence the variation in elastic stiffness due to randomness of ply orientation angle predominantly influence the first three natural frequencies. The relative sensitivity (ratio of sensitivity at a particular speed and total sensitivity) and relative frequencies (ratio of deterministic mean of rotating frequency to stationary frequency) with respect to rotational speeds for first three natural frequencies of eight layered graphite-epoxy angle-ply $[(45^\circ/-45^\circ/45^\circ/-45^\circ)s]$ composite conical shells are furnished in Fig. 7. The relative sensitivity of rotational speeds for first the three natural frequencies are observed to increase with the increase of rotational speeds. A threshold rotational speed is observed below which the relative sensitivity of rotational speeds is found to decrease with increase in number of modes while the reverse trend is identified for the same beyond that threshold rotational speed. This is mainly due to the fact that before the threshold speed, the contribution of the first mode is more than other modes. However, the second and third modes contribution becomes more significant after the threshold speed. The relative frequencies are found to decrease with increase of rotational speeds. As the number

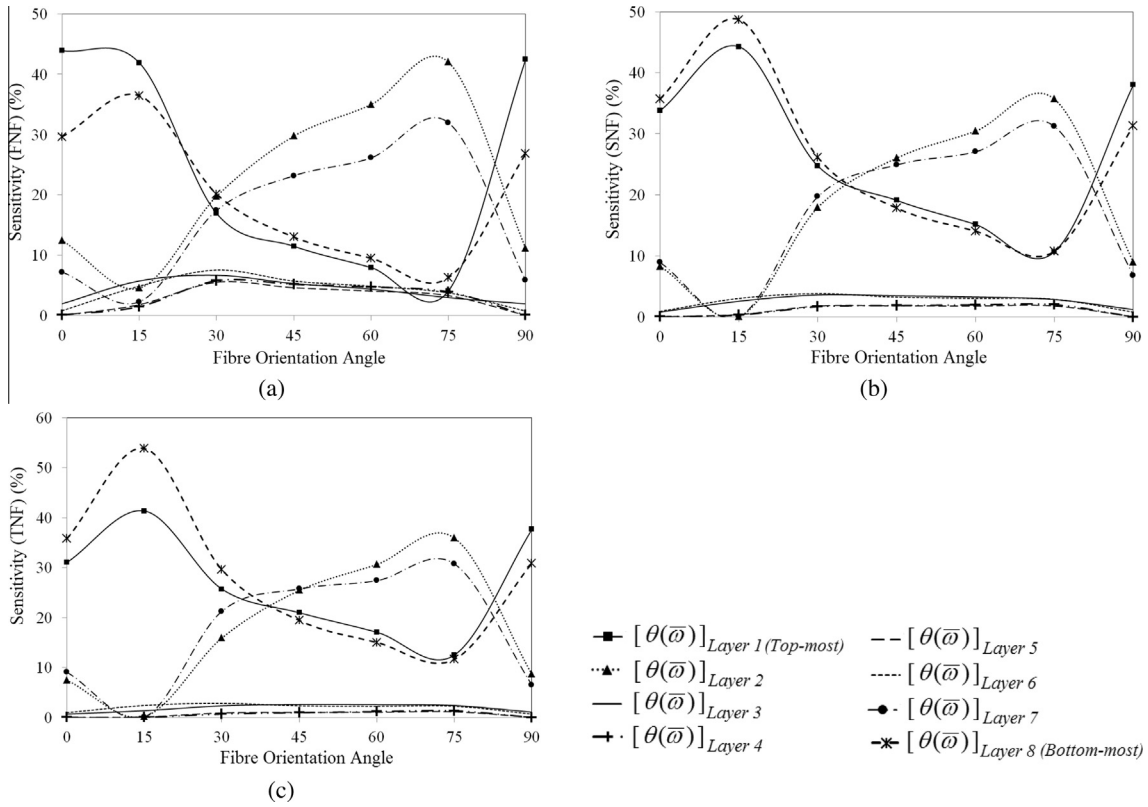

Fig. 6. Sensitivity in percentage for variation in only fiber orientation angle $[\theta(\overline{\omega})]$ ($\pm$ 5° variation) for eight layered graphite-epoxy angle-ply [$(\theta°/-\theta°/\theta°/-\theta°)$s] composite conical shells, considering t = 0.003 m, ν = 0.3, Lo/s = 0.7, ϕ_o = 45°, ϕ_{ve} = 20° (FNF – fundamental natural frequency, SNF – second natural frequency and TNF – Third natural frequency).

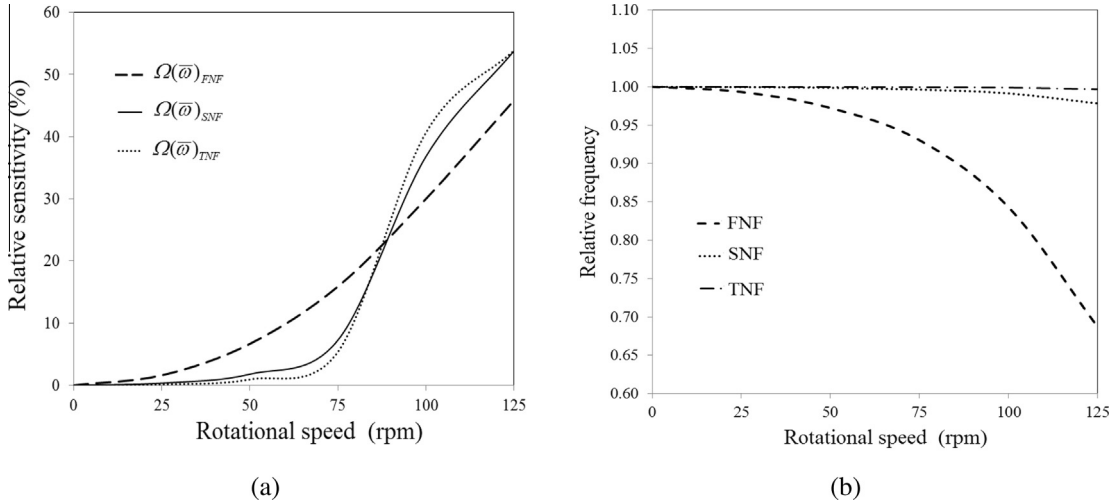

Fig. 7. (a) Relative sensitivity (rotational) and (b) Relative frequency with respect to rotational speed ($\pm$ 10% variation) for eight layered graphite-epoxy angle-ply [(45°/−45°/45°/−45°)s] composite conical shells, considering t = 0.003 m, ν = 0.3, Lo/s = 0.7, ϕ_o = 45°, ϕ_{ve} = 20° (FNF – fundamental natural frequency, SNF – second natural frequency and TNF – Third natural frequency).

of modes increases the rate of decrease of relative frequencies are observed to decrease with increase of rotational speeds. The trend of random fluctuation of rotational speeds are portrayed by probability density function corresponding to first three natural frequencies as furnished in Fig. 8. As the rotational speed increases the stochastic mean of first three natural frequencies are found to decrease whereas the standard deviation of the same are observed to increase with increase of rotational speed. It can be attributed as the coupling effect between geometric stiffness due to rotation and elastic stiffness. Fig. 9 presents the representative difference in deterministic (stationary) and stochastic (rotational) modeshapes considering individual stochasticity in rotational speed wherein the spanwise bending is predominantly observed for first three modes. The significant effect in modeshapes for variation of rotational speeds may occur during real-time operation of such composite structures which is predominantly caused due to its random change in geometric stiffness in addition to its elastic stiffness. The first three natural modes shows the basic bending

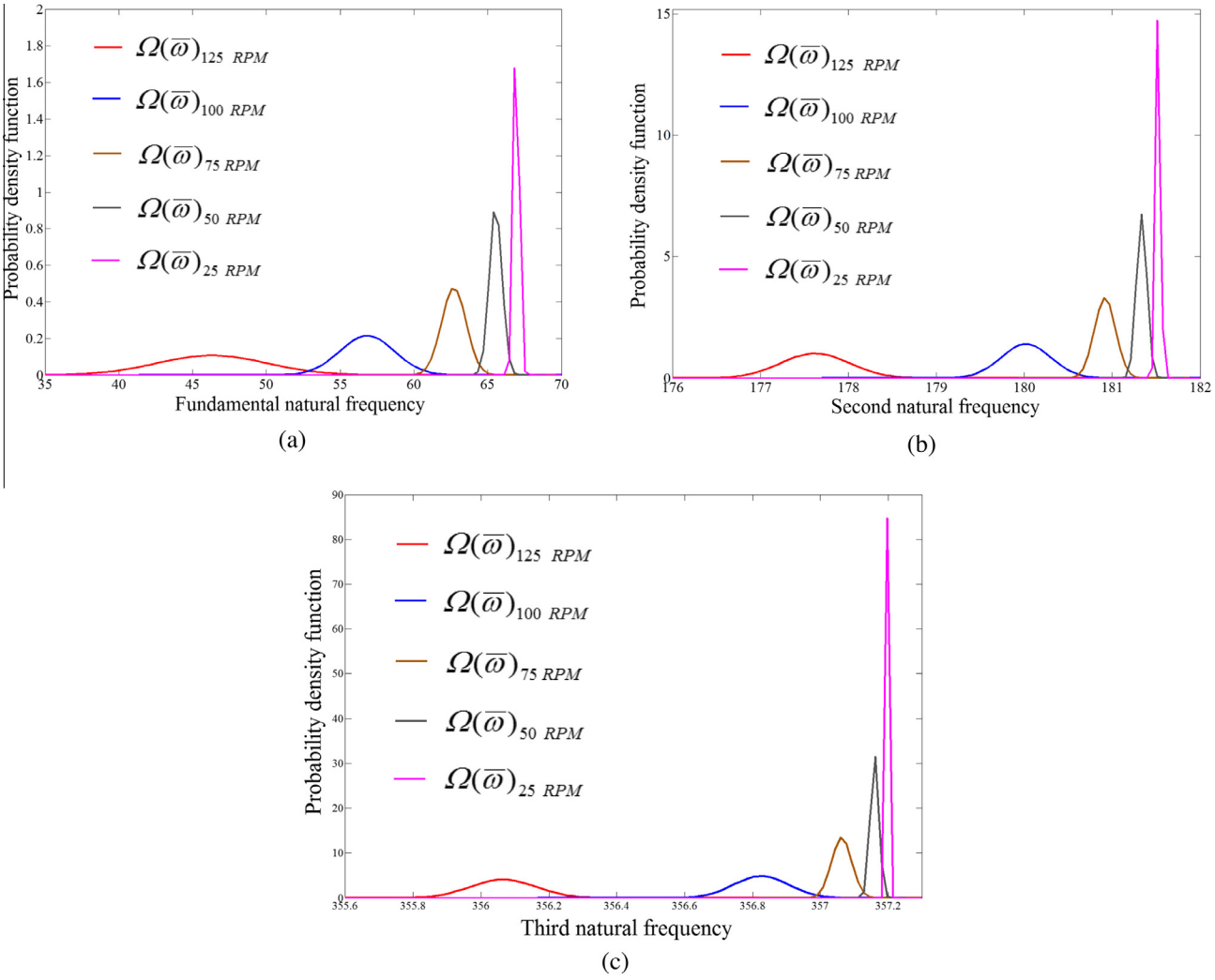

Fig. 8. Probability density function with respect to first three natural frequencies due to only variation in rotational speeds ($\Omega(\overline{\omega})$ = 25, 50,75,100,125 rpm with ± 10% variation) for angle-ply [(45°/−45°/45°/−45°)s] composite conical shells considering t = 0.003 m, ν = 0.3, Lo/s = 0.7, ϕ_o = 45°, ϕ_{ve} = 20°.

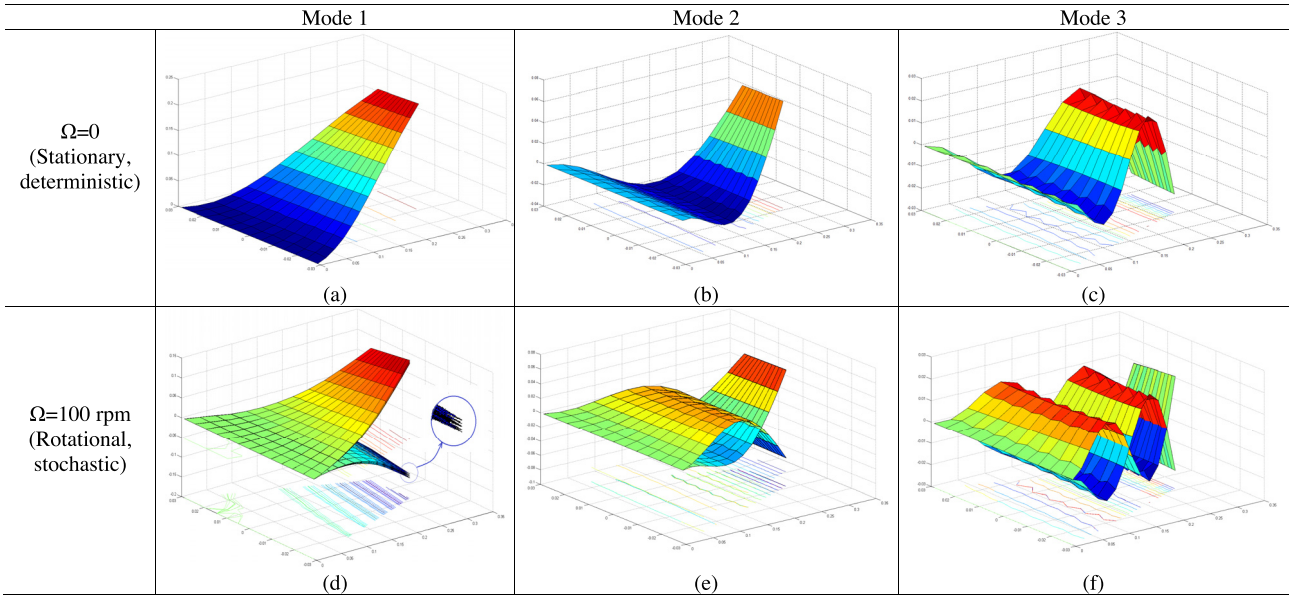

Fig. 9. Modeshapes with respect to first three natural frequencies due to only variation in rotational speeds at $\Omega(\overline{\omega})$ = 100 rpm (± 10% variation) for angle-ply [(45°/−45°/45°/−45°)s] composite conical shells considering t = 0.003 m, ν = 0.3, Lo/s = 0.7, ϕ_o = 45°, ϕ_{ve} = 20°.

modeshapes for deterministic plot without considering any rotation (i.e., stationary case) while stochastic modeshapes with random spanwise bending modes are obtained for random variation of rotational speeds. It is also to be noted that in first mode, a smooth surface is obtained while in case of second and third modes, it shows the wrinkles on the represented surface. These undulations on the surfaces of second and third mode shapes are caused due to consideration of lower mesh size in the present study (6×6 mesh). This problem can be mitigated by using higher mesh size which will lead to higher cost of computation. The present stochastic analysis is carried out with 6×6 mesh size to achieve computational efficiency and accuracy.

5. Conclusions

The novelty of present study includes the individual and combined effect of ply level and rotational uncertainty quantification of first three natural frequencies of composite cantilever conical shells. The number of actual finite element analysis is reduced in the present analysis using central composite design compared to original Monte Carlo simulation and is equal to the number of sample required to construct the CCD model. The results obtained employing CCD are compared with the results of direct Monte Carlo Simulation method and are found to establish the accuracy and computational efficiency. The first three natural frequencies are found to be reduced as the ply orientation angle increases for a particular rotational speed. The ply orientation angles of ultimate and penultimate outer layers are complementarily found to be most sensitive while the middle layers are observed to be least sensitive for first three natural frequencies. The stochastic means of first three natural frequencies are found to decrease as the rotational speed increases while the standard deviations of the same are observed to increase with increase of rotational speed. The relative sensitivity of rotational speeds for first three natural frequencies are observed to increase with the increase of rotational speeds. The relative frequencies are found to decrease with increase of rotational speeds. As the number of modes increases the rate of decrease of relative frequencies are observed to decrease with increase of rotational speeds. The spanwise bending mode is observed to be predominant for first three modes. The future investigation will be carried out to interrogate whether the above conclusions hold true for more complex system.

References

[1] Montgomery DC. Design and analysis of experiments. N.J.: John Wiley and Sons; 1991.
[2] Borkowski JJ. Spherical prediction-variance properties of central composite and Box-Behnken designs. Technometrics 1995;37:399–410.
[3] Myers RH, Montgomery DC. Response surface methodology: process and product optimization using designed experiments. 2nd ed. New York: Wiley; 2002.
[4] Khuri AI, Mukhopadhyay S. Response surface methodology. WIREs Comp Stat 2010;2:128–49. John Wiley & Sons Inc.
[5] Aslan N. Application of response surface methodology and central composite rotatable design for modeling and optimization of a multi-gravity separator for chromite concentration. Powder Technol 2008;185(1):80–6.
[6] Fang SE, Perera R. A response surface methodology based damage identification technique. Smart Mater Struct 2009;18. http://dx.doi.org/10.1088/0964-1726/18/6/065009.
[7] Ahmadi M, Vahabzadeh F, Bonakdarpour B, Mofarrah E, Mehranian M. Application of the central composite design and response surface methodology to the advanced treatment of olive oil processing wastewater using Fenton's peroxidation. J Hazardous Mater 2005;123(1–3):187–95.
[8] Zhu PH, Chen LH. A novel method of dynamic characteristics analysis of machine tool based on unit structure. Sci China Tech Sci 2014;57:1052–62. http://dx.doi.org/10.1007/s11431-014-5524-2.
[9] Tornabene F, Fantuzzi N, Bacciocchi M, Viola E. Accurate inter-laminar recovery for plates and doubly-curved shells with variable radii of curvature using layer-wise theories. Compos Struct 2015;124:368–93.
[10] Hemmatnezhad M, Rahimi GH, Tajik M, Pellicano F. Experimental, numerical and analytical investigation of free vibrational behavior of GFRP-stiffened composite cylindrical shells. Compos Struct 2015;120:509–18.
[11] SofiyevA H, Kuruoglu N. On the solution of the buckling problem of functionally graded truncated conical shells with mixed boundary conditions. Compos Struct 2015;123:282–91.
[12] Tornabene F, Fantuzzi N, Viola E, Batra RC. Stress and strain recovery for functionally graded free-form and doubly-curved sandwich shells using higher-order equivalent single layer theory. Compos Struct 2015;119:67–89.
[13] Xiang X, Guoyong J, Wanyou L, Zhigang L. A numerical solution for vibration analysis of composite laminated conical, cylindrical shell and annular plate structures. Compos Struct 2014;111:20–30.
[14] Tornabene F, Fantuzzi N, Bacciocchi M. The local GDQ method applied to general higher-order theories of doubly-curved laminated composite shells and panels: The free vibration analysis. Compos Struct 2014;116:637–60.
[15] Sanliturk KY, Koruk H. A new triangular composite shell element with damping capability. Compos Struct 2014;118:322–7.
[16] Viola E, Rossetti L, Fantuzzi N, Tornabene F. Static analysis of functionally graded conical shells and panels using the generalized unconstrained third order theory coupled with the stress recovery. Compos Struct 2014;112:44–65.
[17] Sofiyev AH. On the buckling of composite conical shells resting on the Winkler-Pasternak elastic foundations under combined axial compression and external pressure. Compos Struct 2014;113:208–15.
[18] Heydarpour Y, Aghdam MM, Malekzadeh P. Free vibration analysis of rotating functionally graded carbon nanotube-reinforced composite truncated conical shells. Compos Struct 2014;117:187–200.
[19] Tornabene F, Fantuzzi N, Viola E, Carrera E. Static analysis of doubly-curved anisotropic shells and panels using CUF approach, differential geometry and differential quadrature method. Compos Struct 2014;107:675–97.
[20] Tornabene F, Viola E, Fantuzzi N. General higher-order equivalent single layer theory for free vibrations of doubly-curved laminated composite shells and panels. Compos Struct 2013;104:94–117.
[21] Dey S, Mukhopadhyay T, Adhikari S. Stochastic free vibration analyses of composite doubly curved shells – A Kriging model approach. Compos Part B: Eng 2015;70:99–112.
[22] Dey S, Mukhopadhyay T, Haddad Khodaparast H, Adhikari S. Stochastic natural frequencies of composite conical shells. Acta Mechanica 2015. http://dx.doi.org/10.1007/s00707-015-1316-4.
[23] Mehrez L, Doostan A, Moens D, Vandepitte D. Stochastic identification of composite material properties from limited experimental databases, part I: Experimental database construction. Mech Syst Signal Process 2012;27:471–83.
[24] Mehrez L, Doostan A, Moens D, Vandepitte D. Stochastic identification of composite material properties from limited experimental databases, Part II: Uncertainty modelling. Mech Syst Signal Process 2012;27:484–98.
[25] Babuška I, Motamed M, Tempone R. A stochastic multiscale method for the elastodynamic wave equation arising from fiber composites. Comput Methods Appl Mech Eng 2014;276:190–211.
[26] Mao Z, Todd M. Statistical modeling of frequency response function estimation for uncertainty quantification. Mech Syst Signal Process 2013;38(2):333–45.
[27] Sepahvand K, Scheffler M, Marburg S. Uncertainty quantification in natural frequencies and radiated acoustic power of composite plates: Analytical and experimental investigation. Appl Acoust 2015;87:23–9.
[28] Dey S, Mukhopadhyay T, Adhikari S. Stochastic free vibration analysis of angle-ply composite plates – A RS-HDMR approach. Compos Struct 2015;122:526–36.
[29] Jagtap KR, Lal A, Singh BN. Stochastic nonlinear free vibration analysis of elastically supported functionally graded materials plate with system randomness in thermal environment. Compos Struct 2011;93(12):3185–99.
[30] Fang C, Springer GS. Design of composite laminates by a Monte Carlo method. Compos Mater 1993;27(7):721–53.
[31] Stefanou G, Papadrakakis M. Stochastic finite element analysis of shells with combined random material and geometric properties. Comput Methods Appl Mech Eng 2004;193(1–2):139–60.
[32] Sriramula S, Chryssanthopoulos MK. Quantification of uncertainty modelling in stochastic analysis of FRP composites. Compos Part A: Appl Sci Manuf 2009;40(11):1673–84.
[33] Pedronia N, Zioa E, Ferrariob E, Pasanisic A, Coupletc M. Hierarchical propagation of probabilistic and non-probabilistic uncertainty in the parameters of a risk model. Comput Struct 2013;126:199–213.
[34] Zaman K, McDonald M, Mahadevan S. A probabilistic approach for representation of interval uncertainty. Reliab Eng Syst Saf 2011;96(1):117–30.
[35] He Q, Wang J, Liu Y, Dai D, Kong F. Multiscale noise tuning of stochastic resonance for enhanced fault diagnosis in rotating machines. Mech Syst Signal Process 2012;28:443–57.
[36] Piovan MT, Ramirez JM, Sampaio R. Dynamics of thin-walled composite beams: analysis of parametric uncertainties. Compos Struct 2013;105:14–28.
[37] Charmpis DC, Schueller GI, Pellissetti MF. The need for linking micromechanics of materials with stochastic finite elements: a challenge for materials science. Comput. Mater. Sci. 2007;41(1):27–37.
[38] Brampton CJ, Betts DN, Bowen CR, Kim HA. Sensitivity of bistable laminates to uncertainties in material properties, geometry and environmental conditions. Compos Struct 2013;102:276–86.
[39] Salim S, Iyengar NGR, Yadav D. Buckling of laminated plates with random material characteristics. Appl Compos Mater 1998;5:1–9.
[40] Sarangapani G, Ganguli R, Murthy CRL. Spatial wavelet approach to local matrix crack detection in composite beams with ply level material uncertainty. Appl Comp Mater 2013;20:719–46.

[41] Dimitrov N, Friis-Hansen P, Berggreen C. Reliability analysis of a composite wind turbine blade section using the model correction factor method: numerical study and validation. Appl Compos Mater 2013;20:17–39.
[42] Liew KM, Lim CM, Ong LS. Vibration of pretwisted cantilever shallow conical shells. I. J. Solids Struct 1994;31:2463–74.
[43] Meirovitch L. Dynamics and control of structures. New York: John Wiley & Sons; 1992.
[44] Dey S, Karmakar A. Free vibration analyses of multiple delaminated angle-ply composite conical shells – A finite element approach. Compos Struct 2012;94(7):2188–96.
[45] Dey S, Karmakar A. Natural frequencies of delaminated composite rotating conical shells - A finite element approach. Finite Elem Anal Des 2012;56:41–51.
[46] Dey S, Karmakar A. Finite element analyses of bending stiff composite conical shells with multiple delamination. J Mech Mater Struct 2012;7(2):213–24.
[47] Sreenivasamurthy S, Ramamurti V. Coriolis effect on the vibration of flat rotating low aspect ratio cantilever plates. J Strain Anal 1981;16(2):97–106.
[48] Cook RD, Malkus DS, Plesha ME. Concepts and applications of finite element analysis. New York: John Wiley and Sons; 1989.
[49] Bathe KJ. Finite element procedures in engineering analysis. New Delhi: PHI; 1990.
[50] Giunta AA, Wojtkiewicz SF, Eldred MS. Overview of modern design of experiments methods for computational simulations, American Institute of Aeronautics and Astronautics, Paper AIAA 2003-0649; 2003.
[51] Santner TJ, Williams B, Notz W. The design and analysis of computer experiments. Heidelberg: Springer; 2003.
[52] Koehler JR, Owen AB. Computer experiments. In: Ghosh S, Rao CR, editors. Handbook of Statistics, vol. 13. Amsterdam: Elsevier Science B.V.; 1996. p. 61–308.
[53] Slawomir Koziel, Xin-She Yang, editors. Computational Optimization, Methods and Algorithms, Springer, 2011, ISBN: 978-3-642-20858-4 (Print) 978-3-642-20859-1.
[54] Mukhopadhyay T, Dey TK, Dey S, Chakrabarti A. Optimization of fiber reinforced polymer web core bridge deck – A hybrid approach. Struct Eng Int 2015;24(2). http://dx.doi.org/10.2749/101686614X14043795570778.
[55] Mukhopadhyay T, Dey TK, Chowdhury R, Chakrabarti A, Adhikari S. Optimum design of FRP bridge deck: an efficient RS-HDMR based approach. Struct Mult Optim 2015. http://dx.doi.org/10.1007/s00158-015-1251-y.
[56] Jin R, Chen W, Simpson T. Comparative studies of metamodelling techniques under multiple modelling criteria. Struct Multi Optim 2001;23(1):1–13.
[57] Kim BS, Lee YB, Choi DH. Comparison study on the accuracy of metamodeling technique for non-convex functions. J Mech Sci Technol 2009;23(4):1175–81.
[58] Li Y, Ng S, Xie M, Goh T. A systematic comparison of metamodeling techniques for simulation optimization in decision support systems. Appl Soft Comput 2010;10(4):1257–73.
[59] Mukhopadhyay T, Dey TK, Chowdhury R, Chakrabarti A. Structural damage identification using response surface based multi-objective optimization: A comparative study. Arabian J Sci Eng 2015;40(4):1027–44.
[60] Djoudi W, Benissad FA, Bacha SB. Optimization of copper cementation process by iron using central composite design experiments. Chem Eng J 2007;133(1–3):1–6.
[61] Zolgharneina J, Shahmoradia A, Ghasemib JB. Comparative study of Box-Behnken, central composite, and Doehlert matrix for multivariate optimization of Pb (II) adsorption onto Robinia tree leaves. J. Chemom 2013;27:12–20.
[62] Qatu MS, Leissa AW. Natural frequencies for cantilevered doubly-curved laminated composite shallow shells. Compos Struct 1991;17:227–55.